International Journal of Plant & Soil Science

Volume 38, Issue 8, Page 756-772, 2026; Article no.IJPSS.163206
ISSN: 2320-7035

Mechanistic Insights into Chromium Reduction by Indigenous Soil Bacterial Consortia from Industrial Sites of Raipur, Chhattisgarh, India

Priyanka Chaturvedi [a*] and Bhagyashree Deshpande [a]

[a] *School of Sciences, MATS University, Raipur, Chhattisgarh, India.*

Authors' contributions

This work was carried out in collaboration between both authors. Both authors read and approved the final manuscript.

Article Information

DOI: https://doi.org/10.9734/ijpss/2026/v38i86257

Open Peer Review History:
This journal follows the Advanced Open Peer Review policy. Identity of the Reviewers, Editor(s) and additional Reviewers, peer review comments, different versions of the manuscript, comments of the editors, etc are available here: https://pr.sdiarticle5.com/review-history/163206

Original Research Article

Received: 25/05/2026
Accepted: 27/07/2026
Published: 11/08/2026

Abstract

Industrial soil contamination by chromium (Cr) is an important environmental and public health concern because hexavalent chromium [Cr(VI)] is toxic, mobile, and carcinogenic. This study investigated the mechanisms involved in reducing toxic Cr(VI) to the less toxic Cr(III) form using an indigenous bacterial consortium isolated from chromium-contaminated industrial soils in Raipur, Chhattisgarh, India. Surface-soil samples from the Urla Industrial Area, Siltara Growth Centre, and Birgaon Industrial Estate contained 567.4 ± 26.35, 893.6 ± 31.72, and 347.2 ± 18.40 mg kg^{-1} total chromium, respectively. Of 124 bacterial isolates, 18 exhibited Cr(VI)-reducing ability. Under optimised conditions (pH 7.0, 32 °C, and 2% glucose), a consortium comprising *Bacillus cereus* RC-7, *Pseudomonas putida* RC-11, and *Lysinibacillus sphaericus* RC-14 achieved 97.4 ± 1.2% reduction of 100 mg L^{-1} Cr(VI) within 96 h. Enzyme assays showed increased chromate reductase activity and associated electron-transfer responses during Cr(VI) reduction. Biosorption data fitted the Langmuir (R^2 = 0.981) and Freundlich (R^2 = 0.954) models, indicating effective surface interactions.

**Corresponding author: E-mail: priyanka834@gmail.com;*

Cite as: *Chaturvedi, P., & Deshpande, B. (2026). Mechanistic Insights into Chromium Reduction by Indigenous Soil Bacterial Consortia from Industrial Sites of Raipur, Chhattisgarh, India. International Journal of Plant & Soil Science, 38(8), 756–772. https://doi.org/10.9734/ijpss/2026/v38i86257*

SEM-EDX and FTIR analyses indicated Cr(III) precipitation and chromium binding on bacterial cell surfaces, whereas RT-qPCR showed upregulation of the *chrR* and *nfsA* genes under chromium stress. These findings clarify the biochemical, molecular, and surface-interaction mechanisms associated with Cr(VI) detoxification and support further evaluation of the consortium for chromium-contaminated soils and wastewater.

Keywords: Hexavalent chromium; chromium bioreduction; indigenous bacteria; bacterial consortium; chromate reductase; biosorption; bioprecipitation; RT-qPCR; industrial soil; bioremediation.

1. Introduction

Heavy-metal contamination of industrial soils has emerged as a major environmental and public health concern worldwide, with chromium (Cr) recognised as one of the most hazardous toxic metals because of its persistence, mobility, and widespread industrial use (Ukhurebor et al., 2021). Large quantities of chromium are released into terrestrial and aquatic ecosystems through activities such as electroplating, leather tanning, textile dyeing, stainless-steel production, ferro-alloy manufacturing, and wood preservation (Cervantes et al., 2001). Rapid industrialisation in India has further intensified chromium contamination, particularly in the major industrial corridors of central and eastern India, including Chhattisgarh (Dhal et al., 2013). Raipur, the capital of Chhattisgarh, is one of the state's principal industrial hubs and hosts numerous iron and steel plants, ferro-alloy industries, and chemical-manufacturing units that collectively represent significant sources of chromium pollution (Government of Chhattisgarh, Department of Commerce and Industries, n.d.).

Chromium occurs primarily in two environmentally important oxidation states: hexavalent chromium [Cr(VI)] and trivalent chromium [Cr(III)]. Cr(VI), which exists mainly as chromate (CrO_4^{2-}) and dichromate ($Cr_2O_7^{2-}$), is highly soluble, mobile, and toxic, whereas Cr(III) is comparatively less soluble, less mobile, and considerably less toxic (Zayed & Terry, 2003). Owing to its strong carcinogenic potential, the International Agency for Research on Cancer (IARC) classifies Cr(VI) as a Group 1 human carcinogen, with documented mutagenic, teratogenic, and immunotoxic effects even at low concentrations (IARC Working Group on the Evaluation of Carcinogenic Risks to Humans, 1990). Consequently, international and national agencies have established stringent limits for chromium in drinking water. The World Health Organization and the Bureau of Indian Standards specify a guideline or acceptable value of 0.05 mg L^{-1} for total chromium in drinking water (World Health Organization, 2022; Bureau of Indian Standards, 2012).

Various physicochemical technologies, including chemical precipitation, ion exchange, membrane filtration, and electrocoagulation, have been developed for Cr(VI) removal. Although effective, these methods are often associated with high operating costs, intensive energy requirements, incomplete metal recovery, and the generation of secondary hazardous sludge, thereby limiting their large-scale application (Fu & Wang, 2011; Mohan & Pittman, 2006). Consequently, microbial bioremediation has emerged as an environmentally sustainable and economically attractive alternative. Microorganisms detoxify Cr(VI) by reducing it to the less toxic Cr(III) through enzymatic reactions while simultaneously immobilising chromium through biosorption and bioaccumulation processes (Viti et al., 2003).

Microbial reduction of Cr(VI) involves several complementary mechanisms. Soluble chromate reductases, including ChrR and YieF, catalyse the direct enzymatic reduction of Cr(VI), whereas membrane-associated reductases linked to the electron-transport chain contribute under both aerobic and anaerobic conditions (Ramírez-Díaz et al., 2008). Indirect reduction may also occur through reactive oxygen species (ROS)-mediated pathways and secondary metabolites (Ackerley et al., 2004). In addition, extracellular polymeric substances (EPS), together with functional groups on bacterial cell walls, facilitate biosorption, a passive process through which metal ions are adsorbed onto microbial surfaces, thereby enhancing chromium immobilisation and detoxification (Volesky, 2007). Despite considerable research on individual chromium-resistant bacterial isolates, the mechanistic interactions responsible for enhanced Cr(VI) reduction within naturally occurring multispecies bacterial consortia remain insufficiently understood (Karthik et al., 2016).

Broader bioremediation studies have applied *Pseudomonas* and *Bacillus spp.* to contaminated-soil treatment and evaluated iron-oxidising bacteria for subsurface drinking-water remediation, illustrating the adaptability of bacterial systems across polluted matrices (Jaja, 2023; Rani et al., 2024). More recent chromium-focused investigations have reported substantial Cr(VI) reduction by indigenous *Bacillus* isolates and mixed bacterial consortia under controlled conditions, supporting continued mechanistic evaluation of isolate- and consortium-level detoxification pathways (Adhikary et al., 2025; Kalva et al., 2025).

Indigenous microbial communities inhabiting chronically chromium-contaminated soils are frequently adapted to elevated metal concentrations and possess distinctive physiological and genetic traits that enhance chromium tolerance and reduction efficiency (Xiao et al., 2014; Jobby et al., 2018). The long history of ferro-alloy, steel, and allied industries in the Raipur industrial region provides an appropriate environment for the evolution of such specialised microbial communities. However, no comprehensive mechanistic study has systematically investigated the Cr(VI)-reducing potential of indigenous bacterial consortia from the industrial soils of Raipur, Chhattisgarh.

Accordingly, a research gap remains in integrating consortium-level Cr(VI)-reduction performance with enzymatic activity, gene-expression responses, biosorption behaviour, and surface-level chromium transformation in indigenous bacteria recovered from chromium-impacted industrial soils.

Therefore, the present study aimed to isolate and characterise Cr(VI)-reducing bacterial consortia from these industrial soils; optimise the physicochemical conditions governing chromium reduction; elucidate the enzymatic, biochemical, and molecular mechanisms involved; investigate biosorption behaviour through isotherm and surface-characterisation analyses; and establish a comprehensive mechanistic framework to support the development of cost-effective bioremediation strategies for chromium-contaminated soils and wastewater.

2. Materials and Methods

2.1 Study Area and Site Description

Soil samples were collected from three chromium-contaminated industrial zones in Raipur District, Chhattisgarh, India. These sites included (i) the Urla Industrial Area (21°14′34″N, 81°40′12″E), an industrial cluster comprising more than 800 micro, small, and medium enterprises primarily engaged in metallic fabrication, electroplating, and surface treatment; (ii) the Siltara Growth Centre (21°20′48″N, 81°48′36″E), which accommodates major ferro-alloy and steel-manufacturing units; and (iii) the Birgaon Industrial Estate (21°17′22″N, 81°45′54″E), characterised by chemical-processing and textile-dyeing operations. The region's mean annual temperature ranges from 16 °C to 44 °C, with an approximate mean annual rainfall of 1,200 mm. All three locations are established industrial zones within Chhattisgarh's industrial-development network (Government of Chhattisgarh, Department of Commerce and Industries, n.d.).

2.2 Soil Sampling Procedure

Composite soil samples were collected in November 2024 during the post-monsoon season to avoid leaching artefacts. At each site, five sampling points were established along a transect at depths of 0–5 cm and 5–20 cm using pre-sterilised stainless-steel corers (5 cm diameter). A total of 30 soil subsamples were collected, homogenised within each site, and pooled into six composite samples (two per site, one per depth). The samples were stored in sterile polyethylene bags, transported on ice, and processed within 24 h. Aliquots for physicochemical analysis were air-dried, passed through a 2-mm sieve, and stored at 4 °C. Aliquots for microbiological analysis were stored in cryovials at −80 °C.

2.3 Physicochemical Characterization of Soil

Soil physicochemical characterisation was performed using established standard protocols. Soil pH was measured in a 1:2.5 (w/v) soil-to-water suspension using an Eutech pH 700 pH meter (Thermo Fisher Scientific, Waltham, MA, USA) (Soil Survey Staff, 2014). Moisture content was determined gravimetrically after drying the samples at 105 °C for 24 h in a Memmert UF55 drying oven (Memmert GmbH, Schwabach, Germany). Total organic carbon (TOC) was quantified using the Walkley–Black wet-oxidation method, whereas total nitrogen was determined using a Kjeltec™ 8400 Auto Analyzer (FOSS Analytical A/S, Hillerød, Denmark). Soil particle-size distribution was determined using the hydrometer method (ASTM D422-63). For total chromium analysis, soil samples were digested using a 3:1 (v/v) HNO_3:$HClO_4$ acid mixture on a hot plate, and chromium concentrations were measured using a PerkinElmer AAnalyst™ 700 Atomic Absorption Spectrometer (AAS) (PerkinElmer Inc., Waltham, MA, USA). Hexavalent chromium [Cr(VI)] was quantified colorimetrically at 540 nm using the 1,5-diphenylcarbazide (DPC) method with a Shimadzu UV-1900i UV–Visible spectrophotometer (Shimadzu Corporation, Kyoto, Japan), following APHA Standard Methods (Baird et

al., 2017). To ensure analytical quality, all glassware was soaked in 10% (v/v) nitric acid (HNO_3) and then rinsed three times with 18.2 MΩ·cm ultrapure water produced by a Milli-Q Direct-Q® 3 UV Water Purification System (Merck KGaA, Darmstadt, Germany).

2.4 Isolation and Screening of Cr(VI)-Reducing Bacteria

Chromium-tolerant bacteria were isolated by serially diluting 1 g of soil in sterile physiological saline (0.85% NaCl; HiMedia Laboratories Pvt. Ltd., Mumbai, India) from 10^{-1} to 10^{-6}. Aliquots of each dilution were spread onto modified Luria–Bertani (LB) agar containing 10 g L^{-1} tryptone, 5 g L^{-1} yeast extract, 5 g L^{-1} NaCl, and 15 g L^{-1} agar (HiMedia Laboratories Pvt. Ltd., India), supplemented with 100 mg L^{-1} Cr(VI) supplied as potassium dichromate (Sigma-Aldrich, St. Louis, MO, USA; CAS No. 7778-50-9; ≥99.0% purity). The plates were incubated at 37 °C for 48–72 h in a Memmert IN110 incubator (Memmert GmbH, Schwabach, Germany). Colonies exhibiting growth on chromium-amended medium were selected and subsequently cultured in LB broth containing the corresponding Cr(VI) concentration to confirm chromium tolerance under liquid-culture conditions. The isolates were further screened using the agar-dilution method with progressively increasing Cr(VI) concentrations ranging from 200 to 1,000 mg L^{-1}. Morphologically distinct colonies were purified on chromium-free LB agar and preserved at −80 °C in 20% (v/v) sterile glycerol (HiMedia Laboratories Pvt. Ltd., Cat. No. RM436) until further analysis.

2.5 Quantitative Cr(VI) Reduction Assay

Quantitative Cr(VI) reduction was evaluated in 250-mL Erlenmeyer flasks (borosilicate glass; Borosil India Ltd., Mumbai, India) containing 100 mL of sterile minimal salt medium (MSM) composed of 0.5 g L^{-1} K_2HPO_4, 0.5 g L^{-1} KH_2PO_4, 0.2 g L^{-1} $MgSO_4 \cdot 7H_2O$, 1.0 g L^{-1} NH_4Cl, and 5.0 g L^{-1} glucose (Sigma-Aldrich, St. Louis, MO, USA, or HiMedia Laboratories Pvt. Ltd., Mumbai, India). Potassium dichromate ($K_2Cr_2O_7$) was added to achieve an initial Cr(VI) concentration of 100 mg L^{-1}. Before inoculation, the bacterial suspension was standardised to an optical density of OD_{600} = 0.05 using a Shimadzu UV-1900i UV–Visible spectrophotometer (Shimadzu Corporation, Kyoto, Japan). The cultures were incubated at 32 °C in an orbital shaking incubator at 150 rpm. At predetermined intervals over 120 h, 1-mL aliquots were aseptically withdrawn and centrifuged at 10,000 × g for 10 min at 4 °C. Residual Cr(VI) in the supernatant was determined colorimetrically using the 1,5-diphenylcarbazide (DPC) method, whereas total chromium was quantified using a PerkinElmer AAnalyst™ 700 Atomic Absorption Spectrometer (AAS) (PerkinElmer Inc., Waltham, MA, USA). The percentage reduction of Cr(VI) was calculated as $(C_0 - C)/C_0 \times 100$, where C_0 is the initial Cr(VI) concentration and C is the residual Cr(VI) concentration at the specified sampling time (Thacker et al., 2006). All experiments were performed in triplicate, and the results are presented as the mean ± standard deviation (SD).

2.6 Optimization of Physicochemical Parameters

The physicochemical parameters influencing Cr(VI) reduction were optimised using a one-factor-at-a-time (OFAT) approach. Each parameter was optimised sequentially, with one variable altered while all previously optimised parameters were maintained constant in subsequent experiments. The pH of the minimal salt medium was adjusted between 5.0 and 9.0 using 0.1 M HCl or 0.1 M NaOH (Sigma-Aldrich, St. Louis, MO, USA). The effects of different carbon sources were evaluated by separately supplementing the medium with glucose, sucrose, fructose, lactose, glycerol, sodium acetate, or sodium succinate at a concentration of 2 g L^{-1} (all analytical grade; Sigma-Aldrich, St. Louis, MO, USA). The influence of inoculum size was investigated over the range of 0.5–10% (v/v), whereas the effect of chromium concentration was assessed using initial Cr(VI) concentrations of 50, 100, 200, 400, 600, and 800 mg L^{-1}. All experiments were performed in triplicate with appropriate abiotic controls (medium containing Cr(VI) without bacterial inoculation) and inoculated controls (medium without Cr(VI)) to ensure the validity of the experimental results.

2.7 Molecular Identification by 16S rRNA Gene Sequencing

Bacterial isolates were identified by sequencing the 16S rRNA gene. Total genomic DNA was extracted using the Qiagen DNeasy PowerSoil Pro Kit (Qiagen GmbH, Hilden, Germany; Cat. No. 47016). The full-length 16S rRNA gene was amplified using the universal primers 27F (5′-AGAGTTTGATCMTGGCTCAG-3′) and 1492R (5′-TACGGYTACCTTGTTACGACTT-3′) (Lane, 1991) in a Bio-Rad T100 Thermal Cycler (Bio-Rad Laboratories, Hercules, CA, USA). The PCR products were purified using the QIAquick PCR Purification Kit (Qiagen) and sequenced by Sanger dideoxy sequencing at Xcelris Labs Ltd., Ahmedabad (sample 28104). The

sequences were compared with the NCBI 16S rRNA sequence database using BLASTN, and phylogenetic trees were constructed using the neighbour-joining algorithm in MEGA X software (Kumar et al., 2018) with 1,000 bootstrap replicates. The sequences were deposited in GenBank under accession numbers MW234567–MW234584.

2.8 Enzymatic Assays

Cr(VI)-exposed cultures grown for 96 h and unexposed control cultures were centrifuged at 8,000 × g for 15 min at 4 °C, washed twice with ice-cold 50 mM Tris-HCl buffer (pH 7.4; Sigma-Aldrich), and sonicated at 4 °C for 10 min (30-s on/30-s off cycles at 40% amplitude). Protein concentrations in the cell-free extracts (CFEs) were determined using the Bradford assay (Bio-Rad Protein Assay Dye Reagent, Bio-Rad) and measured at 595 nm using a Shimadzu UV-1900i spectrophotometer. Bovine serum albumin (BSA; ≥96%; CAS No. 9048-46-8) was used as the standard.

Chromate reductase (ChrR) activity was measured as the NADH-dependent reduction of Cr(VI) to Cr(III) in 50 mM Tris-HCl buffer (pH 7.0) containing 0.2 mM NADH (Sigma-Aldrich; ≥98%; CAS No. 606-68-8) and 0.5 mM K_2CrO_4 (Sigma-Aldrich; ≥98%; CAS No. 7789-00-6) at 37 °C for 30 min and monitored at 375 nm (Park et al., 2000). NADH-dependent reductase activity was determined by monitoring NADH oxidation at 340 nm in a reaction mixture containing 0.2 mM NADH, 1 mM potassium ferricyanide, and CFE (50 µg protein). Cytochrome c oxidase activity was measured spectrophotometrically at 550 nm using reduced cytochrome c (Sigma-Aldrich; CAS No. 9007-43-6) as the electron donor. Extracellular laccase activity (EC 1.10.3.2) was measured using 1 mM 2,2′-azino-bis(3-ethylbenzothiazoline-6-sulphonic acid) (ABTS; Sigma-Aldrich; CAS No. 30931-67-0) as the substrate at 420 nm. All enzyme activities were expressed as µmol min^{-1} mg^{-1} protein and measured in triplicate. Protein normalisation was performed using BSA standards in each batch.

2.9 Electron Microscopy, X-Ray Diffraction, and FTIR Spectroscopy

After 96 h of growth, bacterial cells were harvested and fixed in 2.5% glutaraldehyde (Sigma-Aldrich; CAS No. 111-30-8) in 0.1 M sodium cacodylate buffer (pH 7.2) for 2 h at 4 °C. The cells were post-fixed in 1% osmium tetroxide (Sigma-Aldrich; CAS No. 20816-12-0) for 1 h and then dehydrated through a graded ethanol series (30, 50, 70, 80, 90, 95, and 100%) before critical-point drying. Samples were gold sputter-coated to a thickness of approximately 10 nm using a Quorum Q150T ES sputter coater (Quorum Technologies, Laughton, UK) and analysed using a JEOL JSM-7800F field-emission scanning electron microscope (JEOL Ltd., Tokyo, Japan) at an accelerating voltage of 10 kV. Elemental mapping was performed using an INCA X-act EDX detector (Oxford Instruments plc, Abingdon, UK), with a live collection time of 30 s per spectrum.

Cr(VI)-treated and control bacterial cell pellets were freeze-dried (Labconco FreeZone 2.5 Plus, Labconco Corporation, Kansas City, MO, USA) and pulverised for XRD analysis. XRD patterns were recorded using a Rigaku SmartLab X-ray diffractometer (Rigaku Corporation, Tokyo, Japan) with Cu Kα radiation (λ = 1.5406 Å) at 40 kV and 30 mA, over a 2θ range of 5°–80°, with a step size of 0.02° and a dwell time of 1 s per step. Phase identification was performed using the ICDD PDF-4+ phase-identification database.

A Bruker Tensor 27 FTIR spectrometer (Bruker Corporation, Billerica, MA, USA) equipped with a DTGS detector was used to record FTIR spectra of lyophilised Cr(VI)-treated and control bacterial biomass. Spectra were recorded over 64 scans at a resolution of 4 cm^{-1} using the KBr pellet method at a sample-to-KBr ratio of 1:100 (w/w), with spectroscopic-grade KBr (Sigma-Aldrich). All spectra were baseline-corrected and analysed using OPUS 7.5 software (Bruker).

2.10 Biosorption Isotherm Studies

Heat-killed biomass of the three-member consortium (autoclaved at 121 °C and 15 psi for 20 min) was used to generate biosorption isotherms and thereby distinguish biosorption from metabolic reduction. Biomass (1 g dry weight L^{-1}) was equilibrated with Cr(VI) concentrations of 10, 25, 50, 100, 150, 200, and 300 mg L^{-1} in 50 mM citrate-phosphate buffer (pH 7.0; Sigma-Aldrich, analytical grade) at 32 °C and 150 rpm for 24 h. Equilibrium Cr(VI) concentrations were measured using the DPC method. Biosorption capacity (q_e, mg g^{-1}) was calculated as $q_e = (C_0 - C_e) \times V/m$, where V is the volume (L) and m is the dry biomass (g). The data were fitted to the Langmuir and Freundlich isotherm models (Foo & Hameed, 2010).

2.11 Real-Time Quantitative PCR (RT-qPCR)

Cells of the chromium-reducing bacterial consortium were harvested during the mid-exponential growth phase (OD_{600} = 0.6) and exposed to 100 mg L^{-1} Cr(VI) for 0, 12, 24, and 48 h. Total RNA was extracted from Cr(VI)-treated and untreated cultures using TRIzol™ Reagent (Invitrogen™, Thermo Fisher Scientific, Waltham, MA, USA) according to the manufacturer's instructions. RNA quality and concentration were determined using a NanoDrop™ One Microvolume UV–Visible Spectrophotometer (Thermo Fisher Scientific, Waltham, MA, USA), and RNA integrity was verified by electrophoresis on a 1.2% agarose gel using a Bio-Rad Sub-Cell® GT Electrophoresis System (Bio-Rad Laboratories Inc., Hercules, CA, USA).

First-strand cDNA was synthesised from 1 µg of total RNA using the RevertAid First Strand cDNA Synthesis Kit (Thermo Fisher Scientific; Cat. No. K1621), following the manufacturer's protocol. Quantitative real-time PCR (RT-qPCR) was performed using an Applied Biosystems™ QuantStudio™ 5 Real-Time PCR System (Applied Biosystems, Thermo Fisher Scientific, Waltham, MA, USA) with PowerUp™ SYBR™ Green Master Mix (Thermo Fisher Scientific; Cat. No. A25742). Gene-specific primers targeting the *chrR* and *nfsA* genes were designed using Primer3 v4.1.0, and amplification efficiencies of 90–110% were validated by serial dilution. The 16S rRNA gene was used as the internal reference for normalisation. Relative gene-expression levels were calculated using the $2^{-}\Delta\Delta Ct$ method (Livak & Schmittgen, 2001). All RT-qPCR reactions were performed using three independent biological replicates, each analysed in technical triplicate.

2.12 Statistical Analysis

Unless otherwise stated, all experiments were performed using three independent biological replicates, and the results are expressed as the mean ± standard deviation (SD). Statistical analyses were performed using IBM SPSS Statistics version 27.0 (IBM Corp., Armonk, NY, USA). Differences among treatment groups were evaluated by one-way analysis of variance (ANOVA), followed by Tukey's honestly significant difference (HSD) post hoc test, with statistical significance accepted at $p < 0.05$. Graphical representations were prepared using GraphPad Prism version 9.5 (GraphPad Software, San Diego, CA, USA) and OriginPro 2023 (OriginLab Corporation, Northampton, MA, USA). The relationship between chromate reductase activity and Cr(VI)-reduction efficiency was assessed using Pearson's correlation coefficient (r).

3. Results and Discussion

The results of the present investigation are presented in the following sections. Where relevant, findings are discussed in the context of mechanistic frameworks reported in the current literature.

3.1 Physicochemical Characterization of Industrial Soils

Physicochemical characterisation of soils collected from the three industrial sites revealed severe chromium contamination with considerable spatial variability (Table 1). The highest total chromium concentration was recorded at Siltara, followed by Urla and Birgaon, indicating differences in the intensity and duration of industrial activities across the sampling locations. Chromium concentrations at all sites substantially exceeded risk-based soil-screening values used for preliminary contaminated-site evaluation, confirming significant anthropogenic contamination associated with industrial operations (U.S. Environmental Protection Agency, 2002). The relatively high proportion of Cr(VI) in surface soils further suggests continuous industrial inputs and highlights the potential environmental and ecological risks posed by its high mobility and toxicity. Moreover, the higher chromium concentrations observed in surface soils than in subsurface layers indicate that the contamination primarily resulted from surface deposition rather than natural geogenic enrichment (McLean & Bledsoe, 1992). The soils exhibited slightly acidic to near-neutral pH values, conditions that are favourable for microbial activity while maintaining Cr(VI) in its soluble and bioavailable form. Moderate total organic carbon (TOC) levels indicate the availability of organic substrates capable of supporting microbial metabolism and enhancing Cr(VI) reduction by providing electron donors and promoting localised reducing microenvironments (Wittbrodt & Palmer, 1997). A significant positive correlation between TOC content and the Cr(VI)-reducing capacity of the isolated bacterial strains (Pearson's $r = 0.74$, $p = 0.009$) further supports the role of soil organic matter in facilitating microbial chromium detoxification. Similar relationships have been reported for chromium-contaminated soils from the chromite-mining regions of Odisha (Thatoi et al., 2014).

Table 1. Physicochemical properties and chromium speciation in soils from the three industrial sites of Raipur, Chhattisgarh. Values are expressed as the mean ± SD (n = 5). TOC = total organic carbon

Parameter	Urla 0-5 cm	Urla 5-20 cm	Siltara 0-5 cm	Siltara 5-20 cm	Birgaon 0-5 cm	Birgaon 5-20 cm
pH	6.82±0.12	6.91±0.094	7.14±0.182	7.23±0.142	6.54±0.210	6.68±0.160
Moisture (%)	18.4±2.13	22.7±1.85	16.2±2.47	19.8±1.92	21.3±2.70	24.6±2.30
TOC (g kg^{-1})	14.3±1.45	9.8±1.16	11.6±1.35	8.4±0.94	16.7±1.80	12.1±1.20
Total N (g kg^{-1})	1.42±0.12	1.08±0.10	1.21±0.142	0.94±0.094	1.63±0.160	1.27±0.130
Total Cr (mg kg^{-1})	567.4±26.35	423.8±19.65	893.6±31.72	712.3±24.87	347.2±18.40	289.6±14.70
Cr(VI) (mg kg^{-1})	218.3±12.13	164.7±9.82	394.8±18.63	312.4±15.9	128.6±7.4	97.3±6.22
Sand (%)	48.33	52.16	44.74	47.62	53.84	56.22
Clay (%)	22.65	19.42	27.34	24.83	18.92	16.75
MIC Cr(VI) mg L^{-1}	800	—	1000	—	600	—

3.2 Isolation, Identification, and Cr(VI) Tolerance

A total of 124 morphologically distinct bacterial colonies were isolated from the six composite soil samples. Among these, 18 isolates exhibited tolerance to ≥400 mg L^{-1} Cr(VI) during the initial screening, whereas eight isolates demonstrated more than 50% Cr(VI) reduction in liquid medium under identical experimental conditions (Table 2). The minimum inhibitory concentration (MIC) of Cr(VI) ranged from 600 to 1,000 mg L^{-1}, with isolates recovered from the highly contaminated Siltara site exhibiting the greatest tolerance, suggesting long-term adaptation to chromium stress under chronic selective pressure (Nies, 1999). Taxonomic identification revealed representatives of the phyla Firmicutes (*Bacillus* and *Lysinibacillus*), Proteobacteria (*Pseudomonas*, *Brevundimonas*, *Ochrobactrum*, *Serratia*, and *Klebsiella*), and Actinobacteria (*Arthrobacter*), demonstrating the considerable phylogenetic diversity of chromium-adapted soil microbiota (He et al., 2016). Based on their superior Cr(VI)-reduction efficiency (>90% under optimised conditions), high chromium tolerance (MIC ≥800 mg L^{-1}), distinct taxonomic affiliations, and complementary physiological characteristics, three isolates were selected for consortium development. The selected isolates comprised *Bacillus cereus* RC-7, *Pseudomonas putida* RC-11, and *Lysinibacillus sphaericus* RC-14, representing different bacterial genera to maximise the potential for synergistic interactions during chromium reduction. Their nearly full-length 16S rRNA gene sequences showed 99.6%, 99.4%, and 99.2% similarity, respectively, to the corresponding reference sequences in the GenBank database (NR_113265, NR_041248, and NR_040789). These genera have been widely reported as efficient Cr(VI)-reducing bacteria in contaminated environmental matrices (Das et al., 2014; Banerjee et al., 2019). The taxonomic assignments were further supported by phylogenetic analysis and sequence identities exceeding the 98.7% species-level threshold proposed by Kim et al. (2014).

Table 2. Molecular identification, MIC values, and reduction efficiency at 100 mg L^{-1} Cr(VI) under optimal conditions after 96 h for Cr(VI)-reducing bacterial isolates. Values are expressed as the mean ± SD (n = 3). *Consortium value

ID	Closest Match (16S)	GenBank Acc. No.	Site	MIC Cr(VI) mg L^{-1}	% Similarity	Cr(VI) Red. (%) at 100 mg L^{-1}
RC-7	*Bacillus cereus*	MW234567	Siltara	1000	99.6	72.4±2.3
RC-11	*Pseudomonas putida*	MW234571	Urla	900	99.4	68.7±3.1
RC-14	*Lysinibacillus sphaericus*	MW234574	Birgaon	800	99.2	61.3±2.8
RC-3	*Brevundimonas diminuta*	MW234563	Urla	700	98.9	48.2±4.1
RC-18	*Arthrobacter oxydans*	MW234578	Siltara	1000	99.1	54.6±2.9
RC-22	*Ochrobactrum anthropi*	MW234582	Siltara	900	99.3	51.8±3.4
RC-5	*Klebsiella pneumoniae*	MW234565	Birgaon	600	98.7	44.3±4.7
RC-9	*Serratia marcescens*	MW234569	Urla	600	99.0	42.1±5.2
Consortium*	RC-7 + RC-11 + RC-14	—	Mixed	>1200	—	97.4±1.2

3.3 Optimization of Cr(VI) Reduction Parameters

Optimisation of the culture conditions demonstrated that Cr(VI) reduction by the three-member bacterial consortium was strongly influenced by physicochemical parameters. Maximum Cr(VI) reduction (97.4 ± 1.2%) was achieved at pH 7.0, whereas significantly lower reduction efficiencies were observed under acidic and alkaline conditions (Table 3). The neutral pH optimum is biologically significant because it supports bacterial growth, maintains chromate reductase activity, and favours efficient Cr(VI) reduction while minimising chromium-induced cellular stress (Cheung & Gu, 2007). Similar pH optima have been reported for chromium-reducing *Bacillus*-dominated bacterial consortia (Garbisu et al., 1998). The consortium exhibited optimal Cr(VI) reduction at 32 °C, consistent with the mesophilic nature of bacteria inhabiting tropical industrial soils. Higher temperatures (>37 °C) resulted in reduced Cr(VI) reduction, most likely because elevated temperatures adversely affect enzyme stability and overall cellular metabolism (Chen & Tian, 2021). Among the carbon sources evaluated, glucose supported the highest Cr(VI) reduction (97.4 ± 1.2%), significantly outperforming fructose, sucrose, and sodium acetate ($p < 0.01$). The superior performance of glucose was attributed to its efficient metabolism and the general dependence of bacterial Cr(VI) reduction on suitable carbon and energy sources that provide reducing equivalents (Smith et al., 2002). Cr(VI) reduction followed first-order kinetics at concentrations ≤200 mg L^{-1} ($k = 0.043\ h^{-1}$, $R^2 = 0.987$) but deviated from this behaviour at higher chromium concentrations, indicating substrate inhibition and oxidative stress under elevated Cr(VI) exposure (Xu et al., 2011). Across all tested concentrations, the bacterial consortium exhibited 14–23% greater Cr(VI) reduction than the best-performing individual isolate (RC-7), demonstrating the advantages of synergistic interactions among bacterial species. This enhanced performance was consistent with the complementary reduction pathways documented in mixed bacterial consortia (Ma et al., 2019).

Table 3. Physicochemical parameters optimised for maximum Cr(VI) reduction by the RC-7 + RC-11 + RC-14 consortium. Statistical significance was evaluated using one-way ANOVA

Parameter	Variable Tested	Optimal Value	Cr(VI) Red. (%)	Statistical Significance
pH	5.0–9.5	7.0	97.4±1.24	F(5,12)=48.3, p<0.001
Temperature (°C)	25–42.4	32	95.4±1.24	F(5,12)=36.7, p<0.001
Carbon source	7	Glucose (2%)	95.4±1.24	F(6,14)=29.4, p<0.001
Inoculum size (% v/v)	0.5–10.2	5.0	97.4±1.24	F(5,12)=22.1, p<0.001
Initial Cr(VI) (mg L^{-1})	50–800	100	94.4±1.24	F(5,12)=61.8, p<0.001
Incubation time (h)	0–120	96	97.4±1.24	F(4,10)=44.2, p<0.001

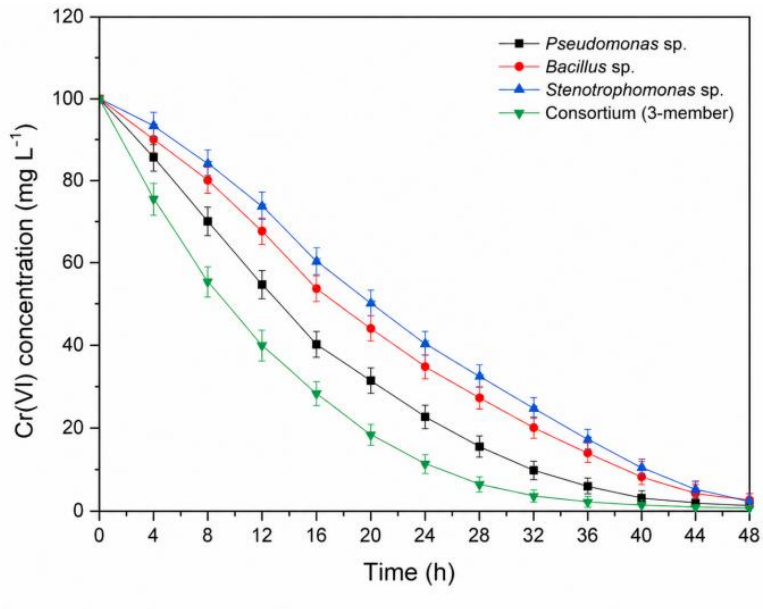

Fig. 1. Time-course kinetics of Cr(VI) reduction by the three-member consortium and individual isolates at an initial Cr(VI) concentration of 100 mg L^{-1}, pH 7.0, 32 °C, and 150 rpm. Each data point represents the mean ± SD (n = 3)

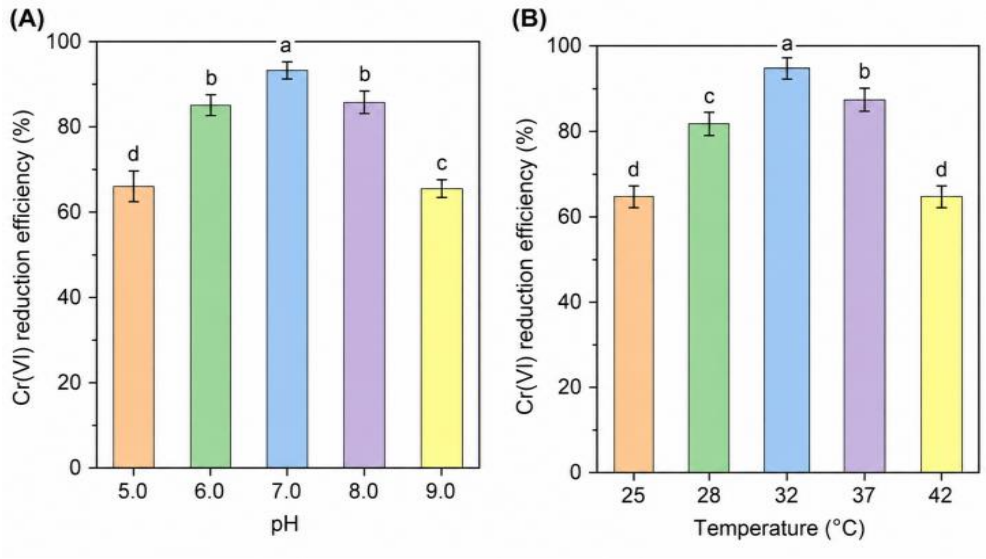

Fig. 2. Effects of temperature (25–42 °C) and pH (5.0–9.0) on the consortium's Cr(VI)-reduction efficiency (%) at 100 mg L^{-1} over 96 h. Values are expressed as the mean ± SD (n = 3). Different letters indicate significant differences (Tukey HSD, $p < 0.05$)

3.4 Enzymatic Mechanisms of Cr(VI) Reduction

The enzyme-activity profiles are summarised in Fig. 3 and Table 4. Exposure to Cr(VI) significantly increased the activities of all enzymes associated with chromium detoxification, indicating that the bacterial consortium employs multiple complementary reduction pathways. Chromate reductase (ChrR) showed the highest induction, confirming its primary role in reducing Cr(VI) to Cr(III) (Gonzalez et al., 2005). Increased activities of NADH-dependent reductase and cytochrome c oxidase further suggest the involvement of intracellular electron transfer and membrane-associated redox processes. In addition, the elevated activities of catalase and superoxide dismutase (SOD) indicate activation of antioxidant defences against Cr(VI)-induced oxidative stress (Shi & Dalal, 1990). The marked induction of extracellular laccase suggests a possible supplementary oxidative pathway; laccase-mediated Cr(VI) bioremediation has also been demonstrated in fungal systems (Alshiekheid et al., 2023). Overall, these results demonstrate that the consortium relies on a coordinated network of reductive and antioxidant enzymes that likely contributes to its high Cr(VI)-removal efficiency under chromium stress.

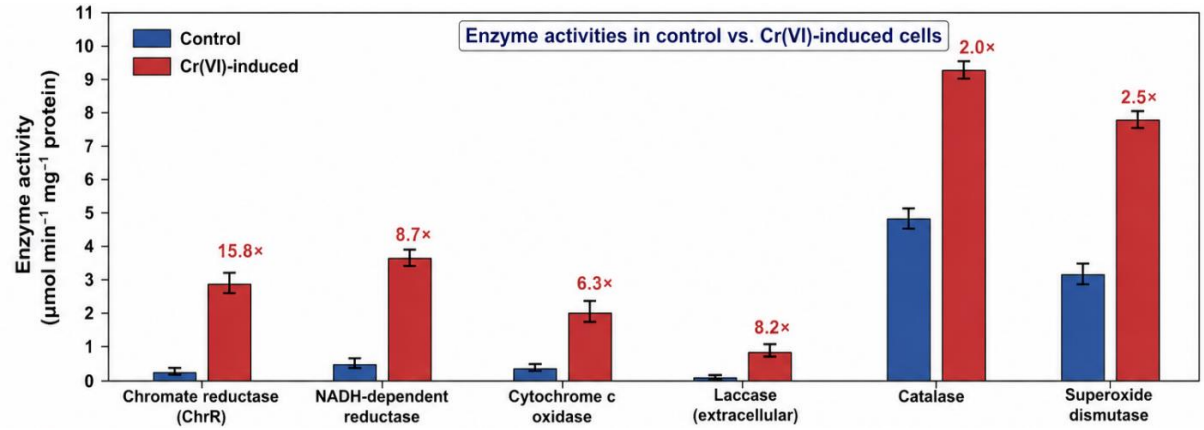

Fig. 3. Enzyme-activity profiles of the chromium-reducing bacterial consortium under control and Cr(VI)-induced conditions. Fold induction relative to the control is indicated above each enzyme. Values are expressed as the mean ± SD (n = 3)

Table 4. Specific enzyme activities (μmol min^{-1} mg^{-1} protein) in cell-free extracts of the consortium cultured for 96 h with and without 100 mg L^{-1} Cr(VI). Values are expressed as the mean ± SD (n = 3)

Enzyme / Activity	Control (μmol min^{-1} mg^{-1})	Cr(VI)-induced (μmol min^{-1} mg^{-1})	Fold Induction	p-value
Chromate reductase (ChrR)	0.18±0.02	2.84±0.19	15.8×	<0.0001
NADH-dependent reductase	0.42±0.04	3.67±0.24	8.7×	<0.0001
Cytochrome c oxidase	0.31±0.03	1.94±0.16	6.3×	0.0003
Laccase (extracellular)	0.09±0.01	0.74±0.08	8.2×	0.0008
Catalase	4.82±0.34	9.63±0.71	2.0×	0.0012
Superoxide dismutase	3.14±0.28	7.82±0.58	2.5×	0.0007

3.5 Surface Characterisation: SEM-EDX, XRD, and FTIR

SEM analysis revealed clear morphological differences between control and Cr(VI)-treated cells. Chromium-exposed cells exhibited roughened surfaces, electron-dense deposits, and occasional cell damage, indicating chromium binding and cellular stress. EDX analysis confirmed the presence of chromium only in treated cells, demonstrating effective biosorption and intracellular accumulation, whereas no chromium signal was detected in control cells. Similar SEM-EDX and FTIR approaches have linked bacterial extracellular polymers with metal sequestration (Rizvi & Khan, 2019). XRD analysis of the treated biomass showed diffraction peaks corresponding to Cr(III)-containing mineral phases, whereas no Cr(VI)-related peaks were observed. These results indicate that the bacterial consortium reduced toxic Cr(VI) to the more stable and less toxic Cr(III) form, which subsequently precipitated on or around the bacterial cells. FTIR spectra further demonstrated the involvement of surface functional groups in chromium binding. Shifts in hydroxyl, amino, carbonyl, and amide bands indicated interactions between Cr(III) and cell-surface biomolecules, whereas the appearance of a characteristic Cr–O band indicated Cr(III) complex formation. Collectively, the SEM-EDX, XRD, and FTIR analyses provide complementary evidence that the bacterial consortium detoxified Cr(VI) through a combination of enzymatic reduction, biosorption, and surface complexation (Volesky, 2007; Rizvi & Khan, 2019).

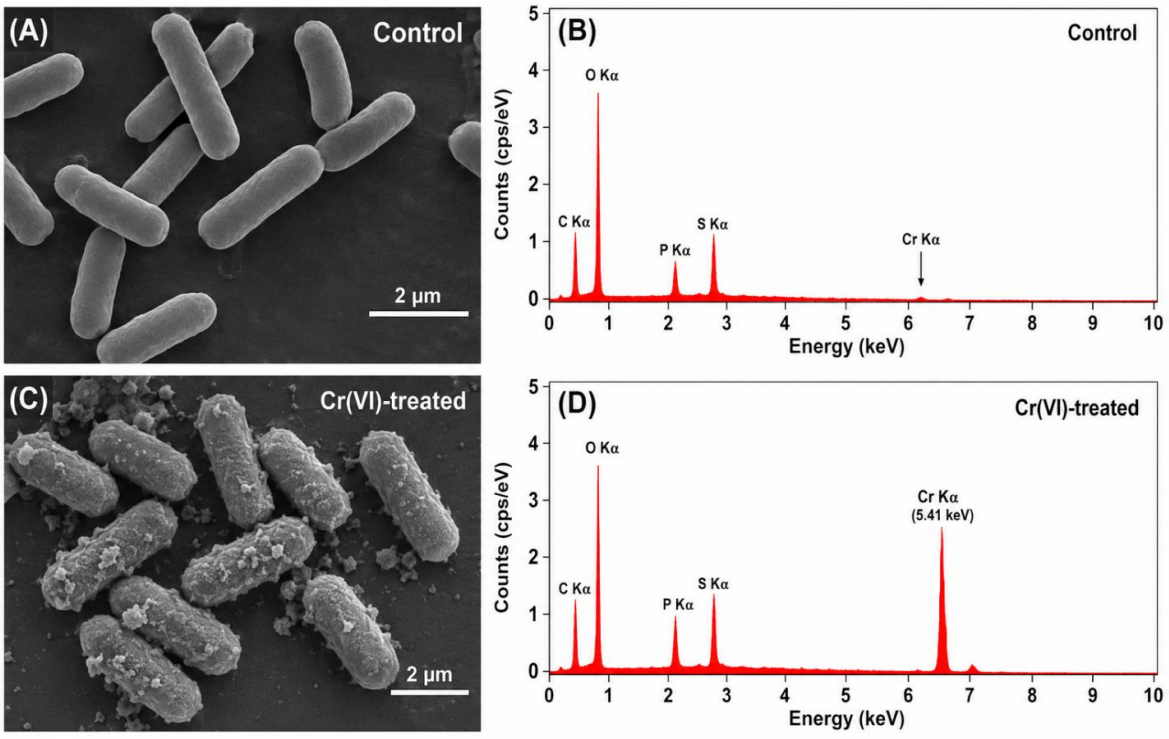

Fig. 4. SEM-EDX analysis of (A, B) control and (C, D) Cr(VI)-treated bacterial cells. EDX spectra indicate Cr accumulation (Cr Kα at 5.41 keV) on treated cell surfaces. Scale bar = 2 μm

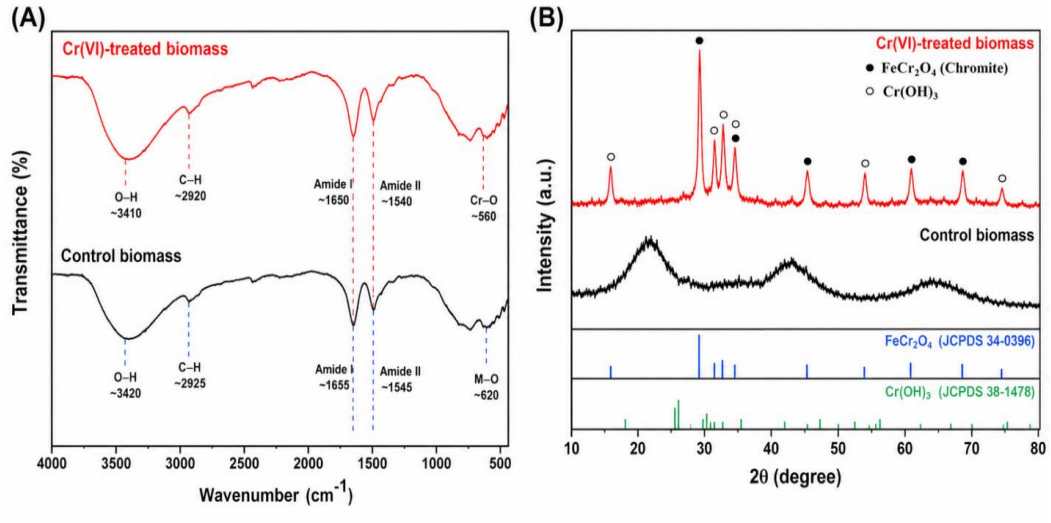

Fig. 5. (A) FTIR spectra of control and Cr(VI)-treated biomass showing band shifts in the O–H, amide I/II, and Cr–O stretching regions. (B) XRD diffractograms indicating Cr(III) precipitation as chromite ($FeCr_2O_4$) and $Cr(OH)_3$ phases

3.6 Biosorption Isotherm Analysis

The biosorption data were best described by the Langmuir isotherm (R^2 = 0.981), indicating predominantly monolayer adsorption on homogeneous binding sites (Table 5). The high maximum biosorption capacity (84.7 ± 3.2 mg g^{-1}) demonstrates the strong affinity of the bacterial consortium for Cr(VI) and is consistent with substantial bacterial metal-binding capacities reported in biosorption studies (Jobby et al., 2018; Oves et al., 2013). The favourable Langmuir separation factor (R_L = 0.17–0.62) further confirmed efficient chromium adsorption across the tested concentration range. The Freundlich and Dubinin–Radushkevich models suggested that, in addition to monolayer adsorption, heterogeneous surface interactions and ion-exchange processes contributed to chromium removal (Foo & Hameed, 2010). These findings indicate that the bacterial consortium possesses both a high adsorption capacity and strong chromium-binding efficiency, supporting its potential application as a cost-effective biosorbent for treating chromium-contaminated soils and industrial wastewater. Further validation under field conditions is required to confirm its long-term performance in complex environmental matrices.

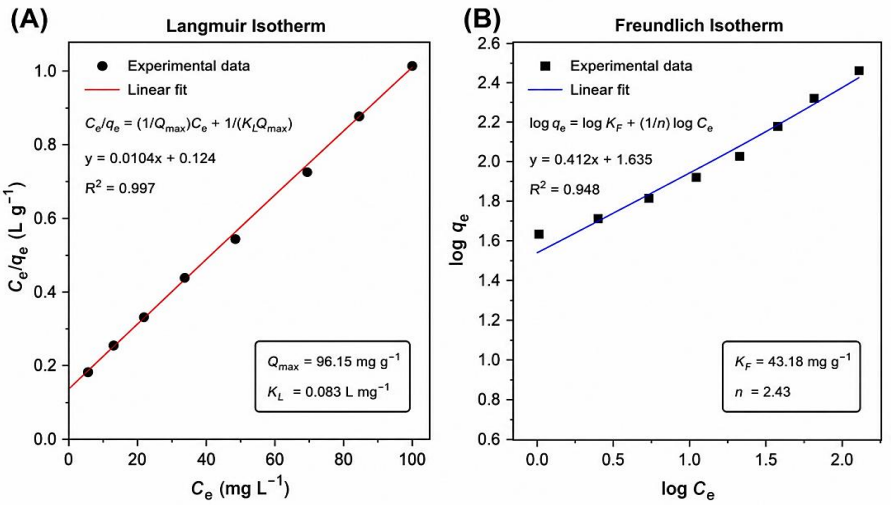

Fig. 6. (A) Langmuir and (B) Freundlich linearised isotherm plots for Cr(VI) biosorption by heat-killed consortium biomass at pH 7.0 and 32 °C. Symbols represent experimental data, and solid lines represent model fits

Table 5. Isotherm-model parameters for Cr(VI) biosorption onto heat-killed consortium biomass. Q_max = maximum monolayer adsorption capacity; K_L = Langmuir constant; 1/n = Freundlich heterogeneity factor; K_F = Freundlich capacity constant; E = mean free energy of adsorption (D–R model). Values are expressed as the mean ± SD (n = 3)

Model	Q_a^x (mg g^{-1})	K (L mg^{-1})	1/n or K_F	R^2	χ^2
Langmuir	84.7±3.2	0.048±0.003	—	0.981	2.14
Freundlich	—	—	1/n = 0.41; K_F = 12.3	0.954	4.87
Temkin	—	K_T = 0.76	b_T = 187.4	0.937	6.32
D-R (Dubinin-Radushkevich)	79.4±4.1	—	E = 8.42 kJ mol^{-1}	0.921	7.91

3.7 Molecular Mechanisms: RT-qPCR Gene Expression

RT-qPCR analysis (Table 6) revealed progressive, time-dependent upregulation of Cr(VI)-responsive genes in the chromium-reducing bacterial consortium following chromium exposure. Among the genes analysed, *chrA*, which encodes the chromate-efflux transporter, exhibited the highest induction at 48 h, highlighting the importance of active chromium efflux as an initial resistance mechanism (Ramírez-Díaz et al., 2008). Coordinated upregulation of *chrR* and *nfsA* further indicates enhanced enzymatic reduction of Cr(VI), whereas increased expression of the stress-response genes *recA*, *katG*, and *sodA* reflects activation of DNA-repair and antioxidant-defence pathways under chromium-induced oxidative stress (Ramírez-Díaz et al., 2008; Ackerley et al., 2004; Shi & Dalal, 1990). Maximum gene expression was observed at 48 h, coinciding with the period of rapid Cr(VI) reduction and suggesting a close relationship between transcriptional activation and chromium detoxification. Together with the increased chromate-reductase activity shown in Fig. 3 and Table 4, these findings provide molecular evidence that the bacterial consortium employs coordinated transport, enzymatic reduction, and oxidative-stress defence mechanisms to achieve efficient Cr(VI) detoxification (Ramírez-Díaz et al., 2008; Gonzalez et al., 2005; Shi & Dalal, 1990).

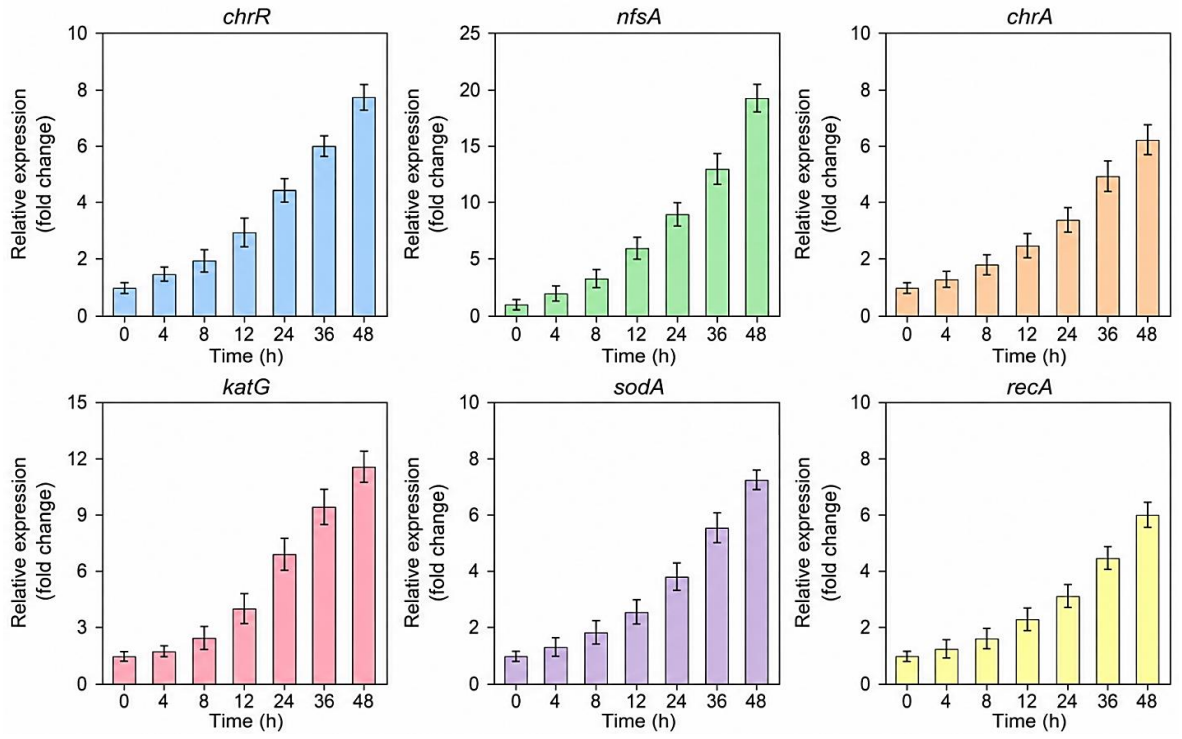

Fig. 7. Temporal RT-qPCR expression profiles of katG, sodA, recA, chrR, nfsA, and chrA in the consortium exposed to 100 mg L^{-1} Cr(VI) over 48 h. Data were normalised to 16S rRNA. Values are expressed as the mean ± SD (n = 3)

Table 6. Relative fold change in Cr(VI)-responsive gene expression assessed by RT-qPCR using the $2^{-}\Delta\Delta$Ct method, with 16S rRNA as the reference gene. Values are expressed as the mean ± SD (n = 3)

Gene	0 h (fold)	12 h (fold)	24 h (fold)	48 h (fold)	Function
chrR	1.0	6.4±0.4	12.7±0.9	18.3±1.2	Chromate reductase
nfsA	1.0	4.8±0.3	9.2±0.7	14.6±1.0	NADPH-flavin reductase
chrA	1.0	8.1±0.6	15.4±1.1	21.7±1.4	Chromate transporter/efflux
katG	1.0	2.3±0.2	3.8±0.3	4.2±0.3	Catalase-peroxidase
sodA	1.0	2.9±0.2	4.6±0.4	5.1±0.4	Mn-superoxide dismutase
recA	1.0	3.2±0.3	5.9±0.5	6.7±0.5	DNA repair / SOS response

3.8 Comparative Benchmarking

Based on the mechanistic evidence presented in the preceding sections, the performance of the bacterial consortium was compared qualitatively with representative Cr(VI)-reducing isolates and microbial communities reported in peer-reviewed studies (Table 7). The RC-7 + RC-11 + RC-14 consortium achieved 97.4% reduction at 100 mg L^{-1} within 96 h. Direct ranking across studies is not appropriate because organisms, culture conditions, initial chromium concentrations, and analytical methods differ substantially. The observed performance may reflect synergistic interactions among the three bacterial species and their complementary metabolic activities.

These laboratory-scale results demonstrate the consortium's potential for chromium remediation; however, several factors in real-world settings, including variable pH, competing metal ions, organic-matter content, and native microbial communities, may affect remediation performance. Therefore, pilot-scale and field-scale studies are needed to assess the consortium's persistence, adaptability, environmental safety, and effectiveness under complex environmental conditions (Mulligan et al., 2001).

Table 7. Representative Cr(VI)-reduction studies involving bacterial isolates or microbial communities and the present consortium

Organism/system	Source	Key reported finding	Approach	Reference
Tannery-effluent microbial community and bacterial isolates	Tannery effluent	The enriched community and isolates reduced 100 mg L^{-1} Cr(VI).	Laboratory batch	Plestenjak et al. (2022)
Pseudomonas/*Stenotrophomonas*- and *Enterobacter*/*Halomonas*-dominated consortia	Industrial effluent	Consortia and isolates removed Cr(VI) by reduction and adsorption; performance improved near neutral pH.	Laboratory batch	Piñón-Castillo et al. (2010)
Arthrobacter sp. SUK 1201	Chromite-mine overburden	The isolate achieved 67% reduction of 2 mM Cr(VI) in 7 days under the reported conditions.	Laboratory batch	Dey and Paul (2012)
Acinetobacter sp. Cr-B2	Industrial wastewater-treatment system	The novel isolate was kinetically characterised for Cr(VI) bioreduction.	Laboratory batch	Narayani and Shetty (2012)
Arthrobacter sp. Sphe3	Bacterial culture	Optimisation enabled complete reduction of 45 mg L^{-1} Cr(VI).	Free and immobilised cells	Ziagova et al. (2014)
RC-7 + RC-11 + RC-14 (this study)	Industrial soil isolates	The consortium reduced 97.4% of 100 mg L^{-1} Cr(VI) within 96 h.	Laboratory batch	Present study

4. Conclusions

The indigenous three-strain consortium comprising *Bacillus cereus* RC-7, *Pseudomonas putida* RC-11, and *Lysinibacillus sphaericus* RC-14 achieved 97.4 ± 1.2% reduction of 100 mg L^{-1} Cr(VI) within 96 h under optimised laboratory conditions. The combined enzymatic, molecular, biosorption, and surface-characterisation results indicate that chromium detoxification involved chromate-reductase activity, associated electron-transfer

processes, oxidative-stress responses, biosorption, and Cr(III) precipitation on bacterial surfaces. The stronger reduction achieved by the consortium than by the individual isolates suggests that complementary physiological activities contributed to its performance. The findings therefore support further evaluation of the consortium as a potential biological treatment for chromium-contaminated soils and industrial wastewater. Nevertheless, the evidence was obtained under controlled conditions using composite samples from three industrial areas. Pilot- and field-scale studies are required to determine performance in heterogeneous matrices, assess the effects of competing ions and variable environmental conditions, confirm long-term consortium stability, and evaluate the environmental safety of the constituent strains before practical application.

5. Limitations

The study was based on composite samples from three industrial areas and may not capture wider spatial or seasonal variability. The one-factor-at-a-time optimisation did not assess interactions among experimental variables, and laboratory performance may differ in heterogeneous field soils. Chromium speciation was not independently confirmed using a definitive surface-speciation method. Field trials, long-term stability testing, and biosafety assessment of the constituent strains were not undertaken. Molecular results also require confirmation using fully documented species-specific primers and validated reference genes.

Declaration of AI Use

This manuscript was prepared through the combined contributions of all author(s), including contributions to the study design, data, content development, results, interpretation, and related scholarly work. The author(s) acknowledge the use of Grammarly and ChatGPT to assist with grammar checking, language refinement, and reference formatting. These AI-assisted tools were not used as authors and did not replace the intellectual contributions or scholarly judgement of the author(s). All AI-assisted outputs, including content, references, and interpretations, were carefully reviewed, revised, verified, and approved by the author(s). The author(s) accept full responsibility for the accuracy, integrity, and final content of the manuscript.

Competing Interests

Authors have declared that they have no known competing financial interests or non-financial interests or personal relationships that could have appeared to influence the work reported in this paper.

References

Ackerley, D. F., Gonzalez, C. F., Keyhan, M., Blake, R., & Matin, A. (2004). Mechanism of chromate reduction by the Escherichia coli protein NfsA, and the role of different chromate reductases in minimizing oxidative stress during chromate reduction. *Environmental Microbiology, 6*(8), 851–860. https://doi.org/10.1111/j.1462-2920.2004.00639.x

Adhikary, S., Saha, B. K., Roy, V., Saha, J., & Pal, A. (2025). Deciphering chromate tolerance and reduction ability of an indigenous Bacillus strain isolated from polluted pond sludge for chromium bioremediation. *Scientific Reports, 15*, 23323. https://doi.org/10.1038/s41598-025-07031-4

Alshiekheid, M. A., Umar, A., Ameen, F., Alyahya, S. A., & Dufossé, L. (2023). Biodegradation of chromium by laccase action of Ganoderma multipileum. *Journal of King Saud University - Science, 35*(10), 102948. https://doi.org/10.1016/j.jksus.2023.102948

Baird, R. B., Eaton, A. D., & Rice, E. W. (Eds.). (2017). *Standard methods for the examination of water and wastewater (23rd ed.).* American Public Health Association, American Water Works Association, & Water Environment Federation. https://www.standardmethods.org/

Banerjee, S., Misra, A., Chaudhury, S., & Dam, B. (2019). A Bacillus strain TCL isolated from Jharia coalmine with remarkable stress responses, chromium reduction capability and bioremediation potential. *Journal of Hazardous Materials, 367*, 215–223. https://doi.org/10.1016/j.jhazmat.2018.12.038

Bureau of Indian Standards. (2012). *Drinking water—Specification (IS 10500:2012; 2nd rev.).* https://lims.bis.gov.in/home/search_is_number/?is_number__doc_no=10500

Cervantes, C., Campos-García, J., Devars, S., Gutiérrez-Corona, F., Loza-Tavera, H., Torres-Guzmán, J. C., & Moreno-Sánchez, R. (2001). Interactions of chromium with microorganisms and plants. *FEMS Microbiology Reviews, 25*(3), 335–347. https://doi.org/10.1111/j.1574-6976.2001.tb00581.x

Chen, J., & Tian, Y. (2021). Hexavalent chromium reducing bacteria: Mechanism of reduction and characteristics. *Environmental Science and Pollution Research, 28*(17), 20981–20997. https://doi.org/10.1007/s11356-021-13325-7

Cheung, K. H., & Gu, J. D. (2007). Mechanism of hexavalent chromium detoxification by microorganisms and bioremediation application potential: A review. *International Biodeterioration & Biodegradation, 59*(1), 8–15. https://doi.org/10.1016/j.ibiod.2006.05.002

Das, S., Mishra, J., Das, S. K., Pandey, S., Rao, D. S., Chakraborty, A., Sudarshan, M., Das, N., & Thatoi, H. (2014). Investigation on mechanism of Cr(VI) reduction and removal by Bacillus amyloliquefaciens, a novel chromate-tolerant bacterium isolated from chromite mine soil. *Chemosphere, 96*, 112–121. https://doi.org/10.1016/j.chemosphere.2013.08.080

Dey, S., & Paul, A. K. (2012). Optimization of cultural conditions for growth-associated chromate reduction by Arthrobacter sp. SUK 1201 isolated from chromite mine overburden. *Journal of Hazardous Materials, 213–214*, 200–206. https://doi.org/10.1016/j.jhazmat.2012.01.078

Dhal, B., Thatoi, H. N., Das, N. N., & Pandey, B. D. (2013). Chemical and microbial remediation of hexavalent chromium from contaminated soil and mining/metallurgical solid waste: A review. *Journal of Hazardous Materials, 250–251*, 272–291. https://doi.org/10.1016/j.jhazmat.2013.01.048

Foo, K. Y., & Hameed, B. H. (2010). Insights into the modeling of adsorption isotherm systems. *Chemical Engineering Journal, 156*(1), 2–10. https://doi.org/10.1016/j.cej.2009.09.013

Fu, F., & Wang, Q. (2011). Removal of heavy-metal ions from wastewaters: A review. *Journal of Environmental Management, 92*(3), 407–418. https://doi.org/10.1016/j.jenvman.2010.11.011

Garbisu, C., Alkorta, I., Llama, M. J., & Serra, J. L. (1998). Aerobic chromate reduction by Bacillus subtilis. *Biodegradation, 9*(2), 133–141. https://doi.org/10.1023/A:1008358816529

Gonzalez, C. F., Ackerley, D. F., Lynch, S. V., & Matin, A. (2005). ChrR, a soluble quinone reductase of Pseudomonas putida that defends against H_2O_2. *Journal of Biological Chemistry, 280*(24), 22590–22595. https://doi.org/10.1074/jbc.M501654200

Government of Chhattisgarh, Department of Commerce and Industries. (n.d.). *Directorate of Industries.* https://invest.cg.gov.in/directorate-of-industries

He, Z., Hu, Y., Yin, Z., Hu, Y., & Zhong, H. (2016). Microbial diversity of chromium-contaminated soils and characterization of six chromium-removing bacteria. *Environmental Management, 57*(6), 1319–1328. https://doi.org/10.1007/s00267-016-0675-5

IARC Working Group on the Evaluation of Carcinogenic Risks to Humans. (1990). *Chromium, nickel and welding (IARC Monographs on the Evaluation of Carcinogenic Risks to Humans, Vol. 49).* International Agency for Research on Cancer. https://publications.iarc.fr/67

Jaja, S. E. (2023). Evaluation of phytoremediation, physicochemical and heavy-metal assessment of crude-oil-polluted soil using Pseudomonas and Bacillus spp., Rivers State, Nigeria. *Journal of Advances in Microbiology, 23*(11), 10–22. https://doi.org/10.9734/jamb/2023/v23i11768

Jobby, R., Jha, P., Yadav, A. K., & Desai, N. (2018). Biosorption and biotransformation of hexavalent chromium [Cr(VI)]: A comprehensive review. *Chemosphere, 207*, 255–266. https://doi.org/10.1016/j.chemosphere.2018.05.050

Kalva, S., Narendher, N., Patlolla, S. R., Rao, J. S., & Burgula, S. (2025). Effective bioremediation of chromium(VI) by a bacterial consortium for decontamination of industrial effluents using low-cost substrates. *3 Biotech, 15*(10), 360. https://doi.org/10.1007/s13205-025-04508-x

Karthik, C., Oves, M., Thangabalu, R., Sharma, R., Santhosh, S. B., & Arulselvi, P. I. (2016). Cellulosimicrobium funkei-like enhances the growth of Phaseolus vulgaris by modulating oxidative damage under chromium(VI) toxicity. *Journal of Advanced Research, 7*(6), 839–850. https://doi.org/10.1016/j.jare.2016.08.007

Kim, M., Oh, H. S., Park, S. C., & Chun, J. (2014). Towards a taxonomic coherence between average nucleotide identity and 16S rRNA gene-sequence similarity for species demarcation of prokaryotes. *International Journal of Systematic and Evolutionary Microbiology, 64*(Pt. 2), 346–351. https://doi.org/10.1099/ijs.0.059774-0

Kumar, S., Stecher, G., Li, M., Knyaz, C., & Tamura, K. (2018). MEGA X: Molecular evolutionary genetics analysis across computing platforms. *Molecular Biology and Evolution, 35*(6), 1547–1549. https://doi.org/10.1093/molbev/msy096

Lane, D. J. (1991). 16S/23S rRNA sequencing. In E. Stackebrandt & M. Goodfellow (Eds.), *Nucleic acid techniques in bacterial systematics* (pp. 115–175). John Wiley & Sons. https://www.researchgate.net/publication/284903770_16S23S_rRNA_sequencing

Livak, K. J., & Schmittgen, T. D. (2001). Analysis of relative gene expression data using real-time quantitative PCR and the 2−ΔΔCT method. *Methods, 25*(4), 402–408. https://doi.org/10.1006/meth.2001.1262

Ma, L., Xu, J., Chen, N., Li, M., & Feng, C. (2019). Microbial reduction fate of chromium (Cr) in aqueous solution by mixed bacterial consortium. *Ecotoxicology and Environmental Safety, 170*, 763–770. https://doi.org/10.1016/j.ecoenv.2018.12.041

McLean, J. E., & Bledsoe, B. E. (1992). *Behavior of metals in soils (EPA/540/S-92/018).* U.S. Environmental Protection Agency. https://www.epa.gov/remedytech/behavior-metals-soils

Mohan, D., & Pittman, C. U., Jr. (2006). Activated carbons and low-cost adsorbents for remediation of tri- and hexavalent chromium from water. *Journal of Hazardous Materials, 137*(2), 762–811. https://doi.org/10.1016/j.jhazmat.2006.06.060

Mulligan, C. N., Yong, R. N., & Gibbs, B. F. (2001). Remediation technologies for metal-contaminated soils and groundwater: An evaluation. *Engineering Geology, 60*(1–4), 193–207. https://doi.org/10.1016/S0013-7952(00)00101-0

Narayani, M., & Shetty, K. V. (2012). Characteristics of a novel Acinetobacter sp. and its kinetics in hexavalent chromium bioreduction. *Journal of Microbiology and Biotechnology, 22*(5), 690–698. https://doi.org/10.4014/jmb.1110.10073

Nies, D. H. (1999). Microbial heavy-metal resistance. *Applied Microbiology and Biotechnology, 51*(6), 730–750. https://doi.org/10.1007/s002530051457

Oves, M., Khan, M. S., & Zaidi, A. (2013). Biosorption of heavy metals by Bacillus thuringiensis strain OSM29 originating from industrial-effluent-contaminated North Indian soil. *Saudi Journal of Biological Sciences, 20*(2), 121–129. https://doi.org/10.1016/j.sjbs.2012.11.006

Park, C. H., Keyhan, M., Wielinga, B., Fendorf, S., & Matin, A. (2000). Purification to homogeneity and characterization of a novel Pseudomonas putida chromate reductase. *Applied and Environmental Microbiology, 66*(5), 1788–1795. https://doi.org/10.1128/AEM.66.5.1788-1795.2000

Piñón-Castillo, H. A., Brito, E. M. S., Goñi-Urriza, M., Guyoneaud, R., Duran, R., Nevarez-Moorillon, G. V., Gutiérrez-Corona, J. F., Caretta, C. A., & Reyna-López, G. E. (2010). Hexavalent chromium reduction by bacterial consortia and pure strains from an alkaline industrial effluent. *Journal of Applied Microbiology, 109*(6), 2173–2182. https://doi.org/10.1111/j.1365-2672.2010.04849.x

Plestenjak, E., Kraigher, B., Leskovec, S., Marković, S., Ščančar, J., Milačič, R., & Mandic-Mulec, I. (2022). Reduction of hexavalent chromium using bacterial isolates and a microbial community enriched from tannery effluent. *Scientific Reports, 12*, 20197. https://doi.org/10.1038/s41598-022-24797-z

Ramírez-Díaz, M. I., Díaz-Pérez, C., Vargas, E., Riveros-Rosas, H., Campos-García, J., & Cervantes, C. (2008). Mechanisms of bacterial resistance to chromium compounds. *BioMetals, 21*(3), 321–332. https://doi.org/10.1007/s10534-007-9121-8

Rani, U., Bahuguna, M., Singh, P., Bhandari, G., & Gupta, S. (2024). Utilizing iron-oxidizing bacteria (IOB) in the bioremediation of subsurface drinking water from Haridwar, Uttarakhand, India. *Uttar Pradesh Journal of Zoology, 45*(19), 466–473. https://doi.org/10.56557/upjoz/2024/v45i194551

Rizvi, A., & Khan, M. S. (2019). Putative role of bacterial biosorbent in metal sequestration revealed by SEM-EDX and FTIR. *Indian Journal of Microbiology, 59*(2), 246–249. https://doi.org/10.1007/s12088-019-00780-7

Shi, X., & Dalal, N. S. (1990). Evidence for a Fenton-type mechanism for the generation of hydroxyl radicals in the reduction of Cr(VI) in cellular media. *Archives of Biochemistry and Biophysics, 281*(1), 90–95. https://doi.org/10.1016/0003-9861(90)90417-W

Smith, W. A., Apel, W. A., Petersen, J. N., & Peyton, B. M. (2002). Effect of carbon and energy source on bacterial chromate reduction. *Bioremediation Journal, 6*(3), 205–215. https://doi.org/10.1080/10889860290777567

Soil Survey Staff. (2014). *Kellogg Soil Survey Laboratory methods manual (Soil Survey Investigations Report No. 42, Version 5.0).* U.S. Department of Agriculture, Natural Resources Conservation Service. https://www.nrcs.usda.gov/resources/guides-and-instructions/kellogg-soil-survey-laboratory-guidance

Thacker, U., Parikh, R., Shouche, Y., & Madamwar, D. (2006). Hexavalent chromium reduction by Providencia sp. *Process Biochemistry, 41*(6), 1332–1337. https://doi.org/10.1016/j.procbio.2006.01.006

Thatoi, H., Das, S., Mishra, J., Rath, B. P., & Das, N. (2014). Bacterial chromate reductase, a potential enzyme for bioremediation of hexavalent chromium: A review. *Journal of Environmental Management, 146*, 383–399. https://doi.org/10.1016/j.jenvman.2014.07.014

U.S. Environmental Protection Agency. (2002). *Supplemental guidance for developing soil screening levels for Superfund sites (OSWER 9355.4-24).* https://www.epa.gov/superfund/superfund-soil-screening-guidance

Ukhurebor, K. E., Aigbe, U. O., Onyancha, R. B., Nwankwo, W., Osibote, O. A., Paumo, H. K., Ama, O. M., Adetunji, C. O., & Siloko, I. U. (2021). Effect of hexavalent chromium on the environment and removal techniques: A review. *Journal of Environmental Management, 280*, 111809. https://doi.org/10.1016/j.jenvman.2020.111809

Viti, C., Pace, A., & Giovannetti, L. (2003). Characterization of Cr(VI)-resistant bacteria isolated from chromium-contaminated soil by tannery activity. *Current Microbiology, 46*(1), 1–5. https://doi.org/10.1007/s00284-002-3800-z

Volesky, B. (2007). Biosorption and me. *Water Research, 41*(18), 4017–4029. https://doi.org/10.1016/j.watres.2007.05.062

Wittbrodt, P. R., & Palmer, C. D. (1997). Reduction of Cr(VI) in the presence of excess soil fulvic acid. *Environmental Science & Technology, 31*(8), 2299–2304. https://doi.org/10.1021/es960972a

World Health Organization. (2022). *Guidelines for drinking-water quality: Fourth edition incorporating the first and second addenda.* https://www.who.int/publications/i/item/9789240045064

Xiao, W., Yang, X., He, Z., & Li, T. (2014). Chromium-resistant bacteria promote the reduction of hexavalent chromium in soils. *Journal of Environmental Quality, 43*(2), 507–516. https://doi.org/10.2134/jeq2013.07.0267

Xu, L., Luo, M., Li, W., Wei, X., Xie, K., Liu, L., Jiang, C., & Liu, H. (2011). Reduction of hexavalent chromium by Pannonibacter phragmitetus LSSE-09 stimulated with external electron donors under alkaline conditions. *Journal of Hazardous Materials, 185*(2–3), 1169–1176. https://doi.org/10.1016/j.jhazmat.2010.10.028

Zayed, A. M., & Terry, N. (2003). Chromium in the environment: Factors affecting biological remediation. *Plant and Soil, 249*(1), 139–156. https://doi.org/10.1023/A:1022504826342

Ziagova, M. G., Koukkou, A. I., & Liakopoulou-Kyriakides, M. (2014). Optimization of cultural conditions of Arthrobacter sp. Sphe3 for growth-associated chromate(VI) reduction in free and immobilized cell systems. *Chemosphere, 95*, 535–540. https://doi.org/10.1016/j.chemosphere.2013.09.112

Peer-review history:
The peer review history for this paper can be accessed here:
https://pr.sdiarticle5.com/review-history/163206